Supplemental Information for:
The Influence of Shallow Subsurface Properties on Particle Motion in Acoustic–Seismic Coupling

Logan T. Scamfer * [1], **David Fee** [1], **Jordan W. Bishop** [2], **Matthew Haney** [3], **Kenneth Macpherson** [1]

[1]Wilson Alaska Technical Center, Geophysical Institute, University of Alaska Fairbanks, Fairbanks, AK, USA, [2]Los Alamos National Laboratory, Los Alamos, NM, USA, [3]United States Geological Survey, Alaska Volcano Observatory, Anchorage, AK, USA

File Contents

This supplementary material includes the following:

- **Supplemental Figures:** Figures S1-S7.

*Corresponding author: ltscamfer@alaska.edu

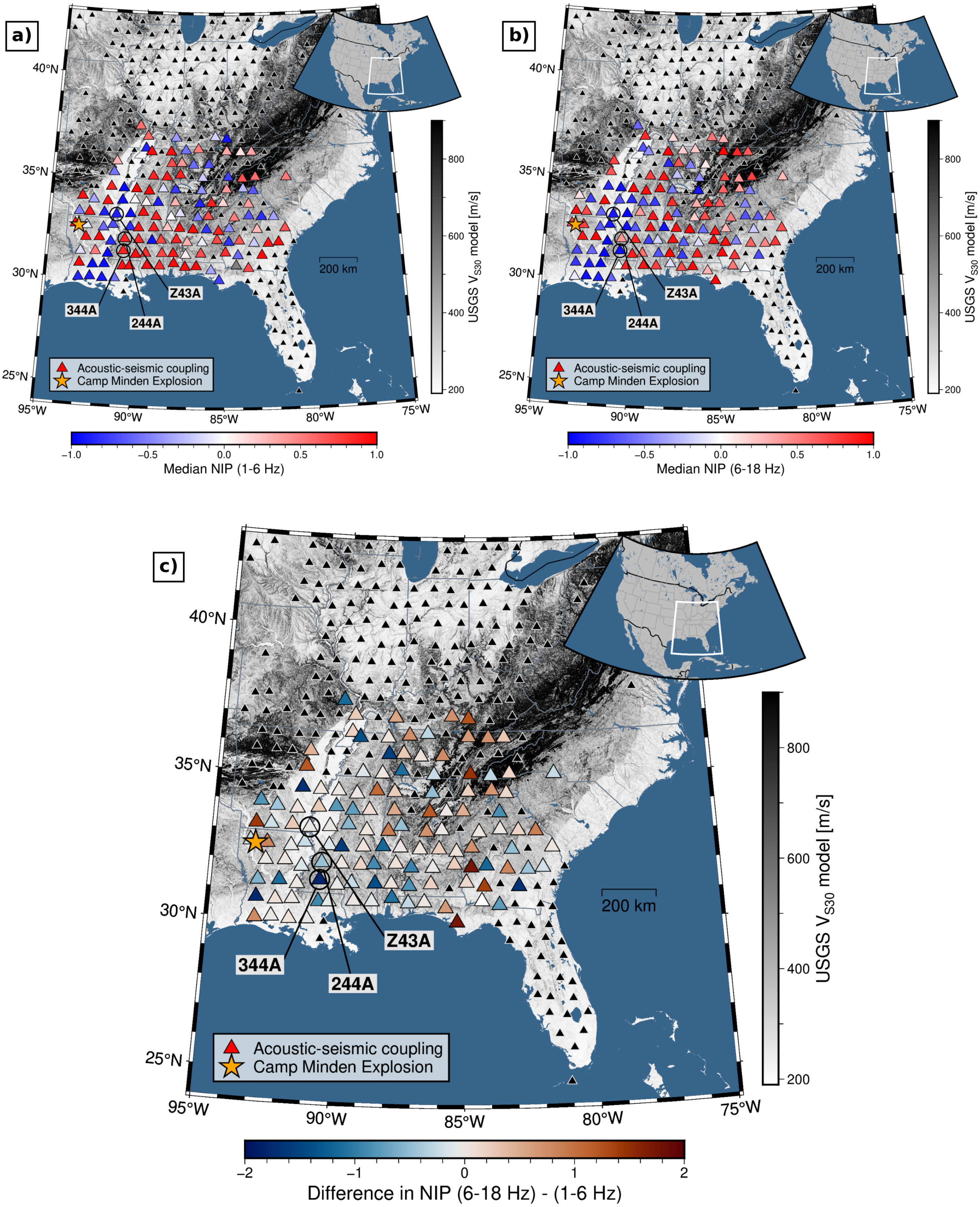

Figure S1 Spatial distribution of air-to-ground coupled wave particle motion from the 2012 Camp Minden Explosion, in two frequency bands: **a)** 1–6 Hz and **b)** 6–18 Hz, while **c)** shows the difference between these two, highlighting frequency-dependent changes in particle motion. Here the blue stations indicate a particle motion transition from retrograde at low frequencies to prograde at higher frequencies, whereas maroon indicates the opposite. White stations show no overall change in particle motion between the different bands.

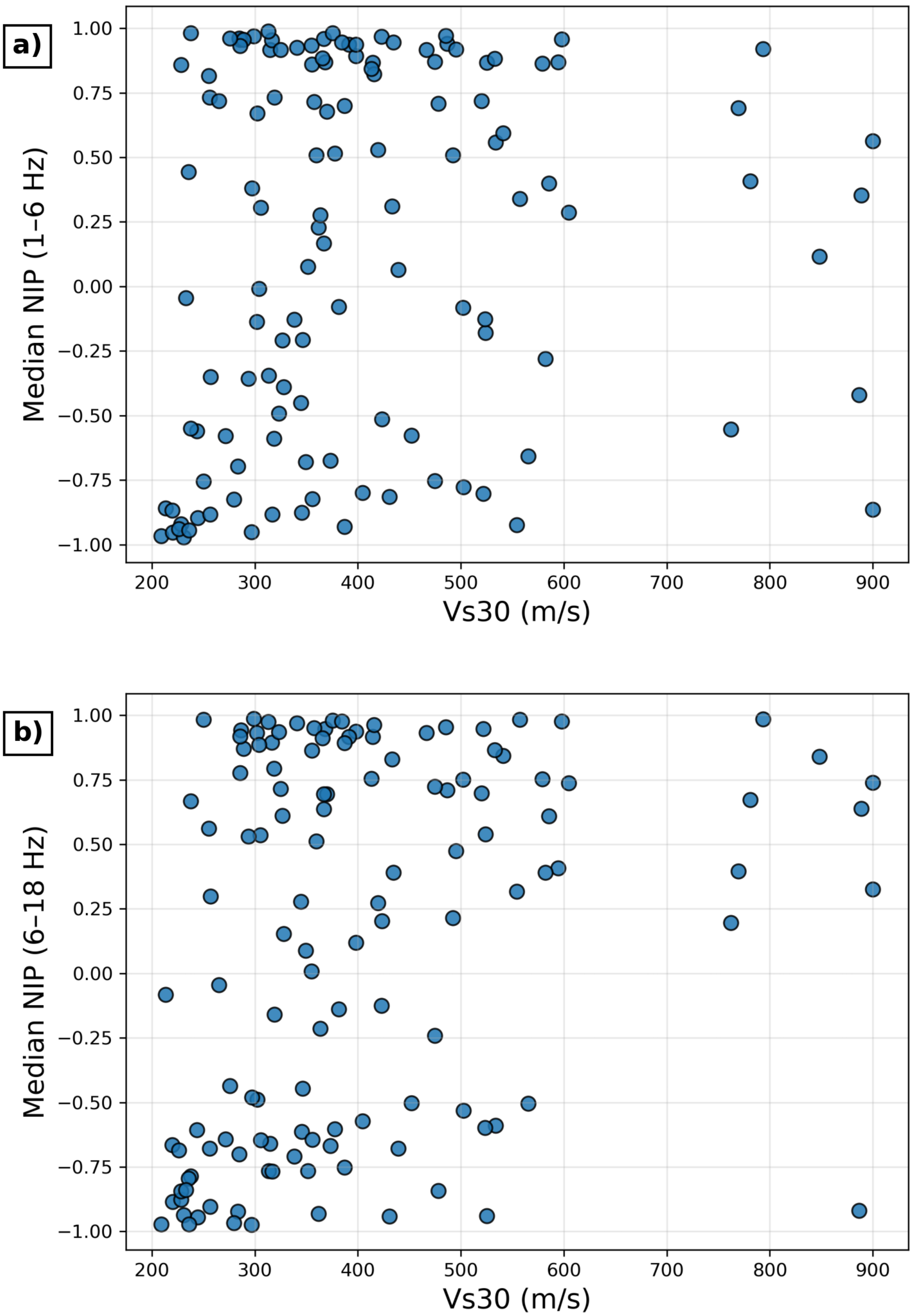

Figure S2 Scatter plot of the station-specific median NIP and the USGS V_{S30} value at the location of each respective station. Each blue circle represents a TA station that recorded acoustic-seismic coupling. Panel **a)** shows the 1–6 Hz frequency band, and panel **b)** shows the 6–18 Hz band.

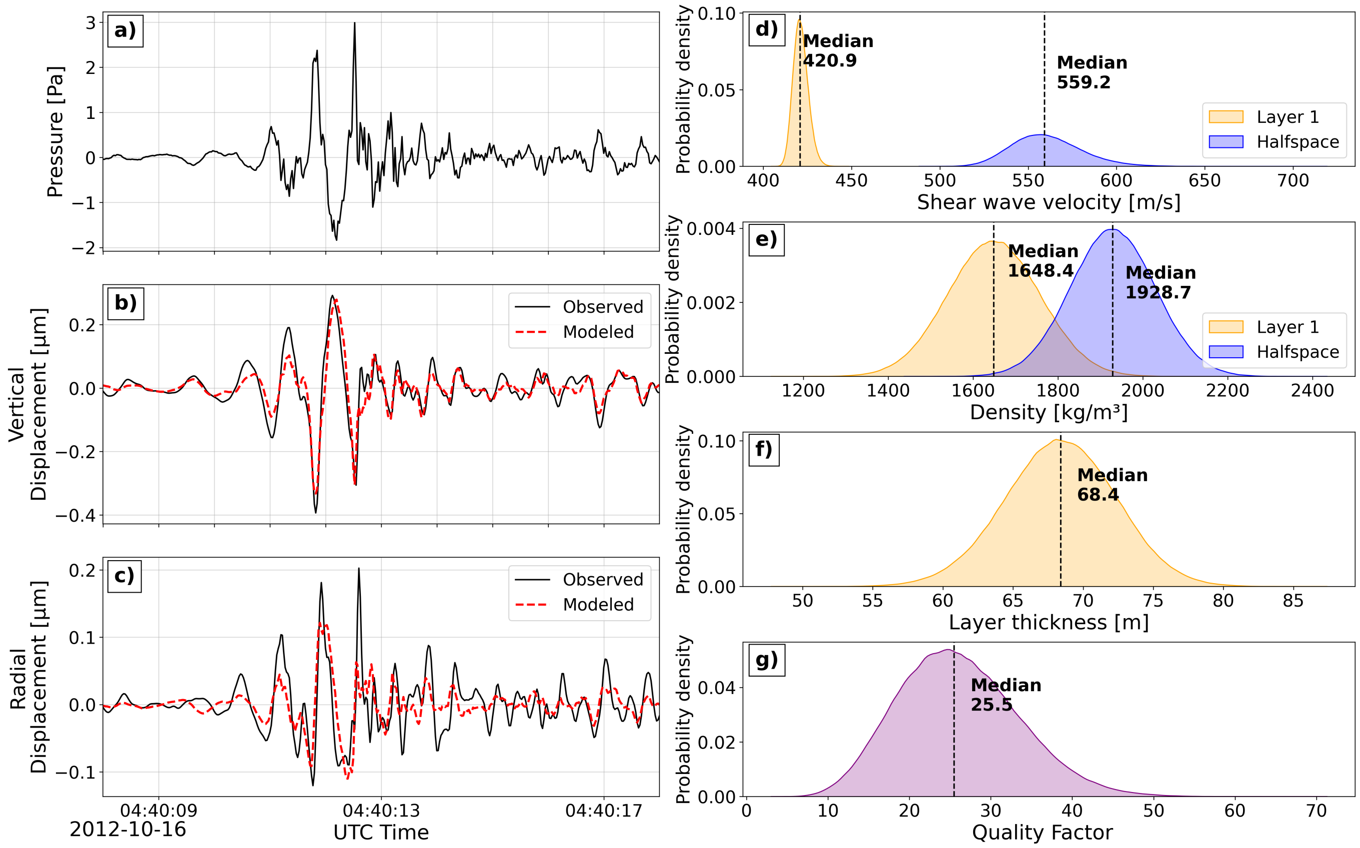

Figure S3 Inversion results at station TA.244A for subsurface properties, including Q_μ as a parameter. The inversion results are largely unaffected by the inclusion of Q_μ, as there is little to no difference is observed in the waveform fit or the median posterior parameters compared to the results without Q_μ in Figure 6 in the main text.

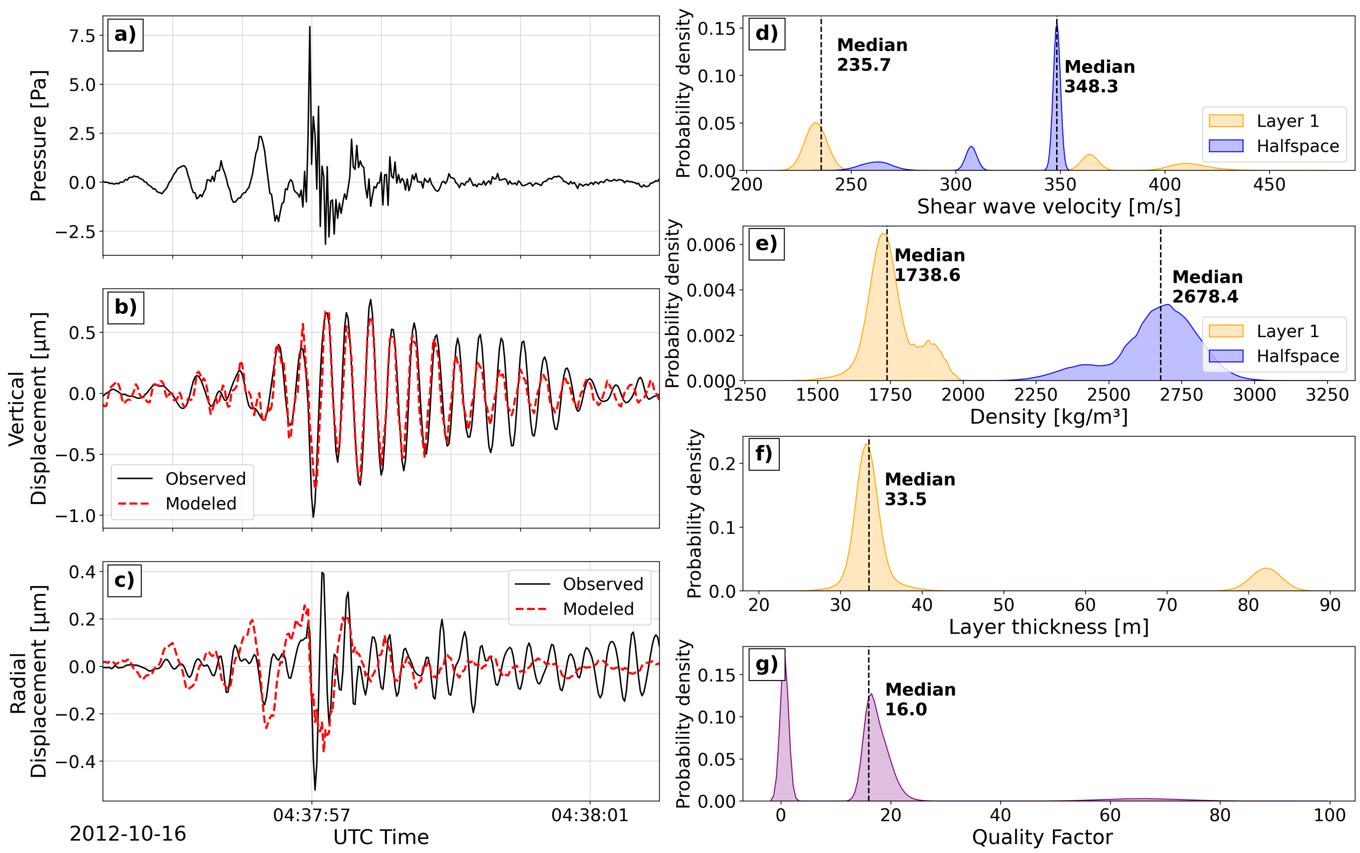

Figure S4 Inversion results at station TA.Z43A for subsurface properties, including Q_μ as a parameter. The inversion results are largely unaffected by Q_μ, as there is little to no difference is observed in the waveform fit or the median posterior parameters compared to the results without Q_μ in Figure 8 in the main text.

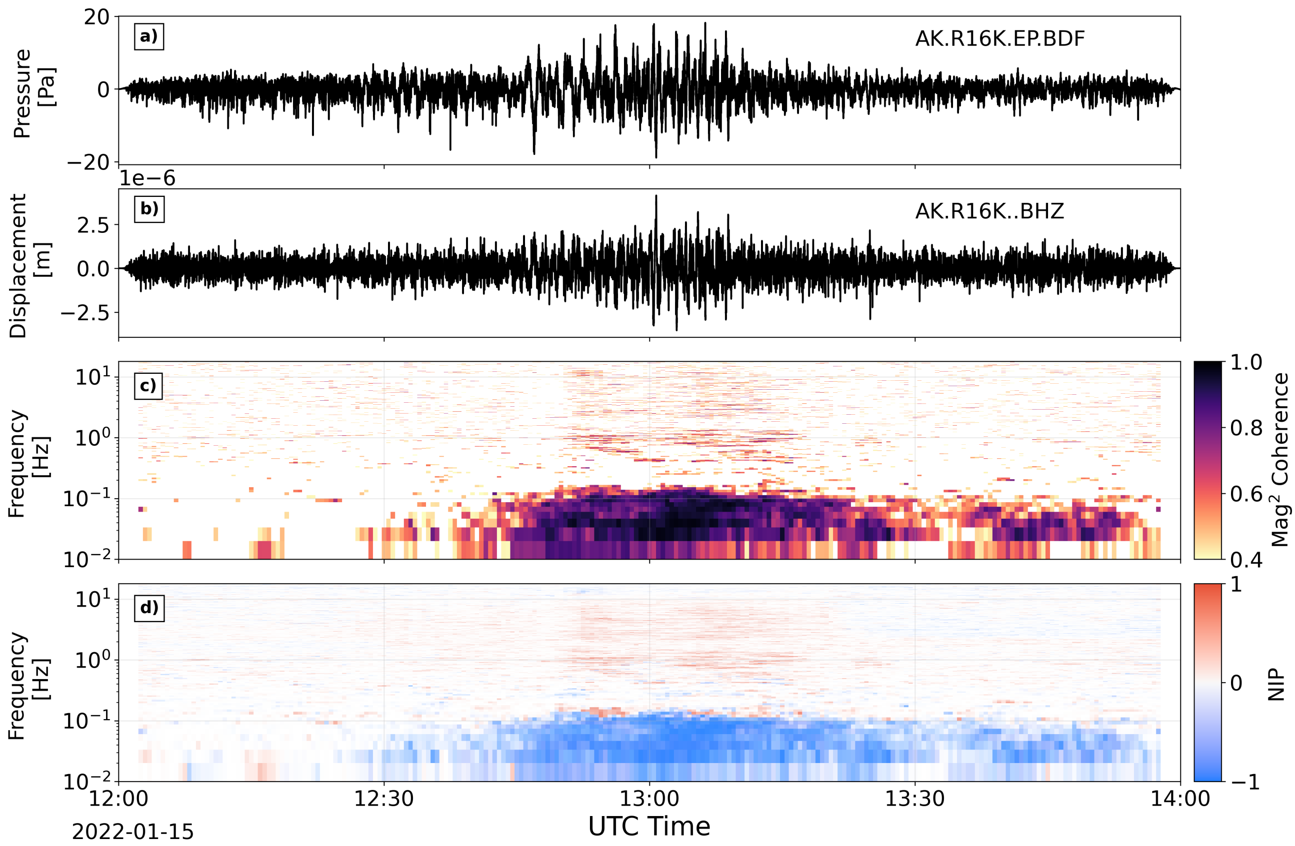

Figure S5 Air-to-ground coupled infrasound from the eruption of Hunga, Tonga volcano at station AK.R16K, located at Pilot Point, Alaska. Panels contents are the same as the left column in Figures 3, 4, and 5 in the main text. For this analysis we use 300 s sliding windows with 90 % overlap. Prograde particle motion is seen at very low frequencies (0.01–0.15) in panel **d)**.

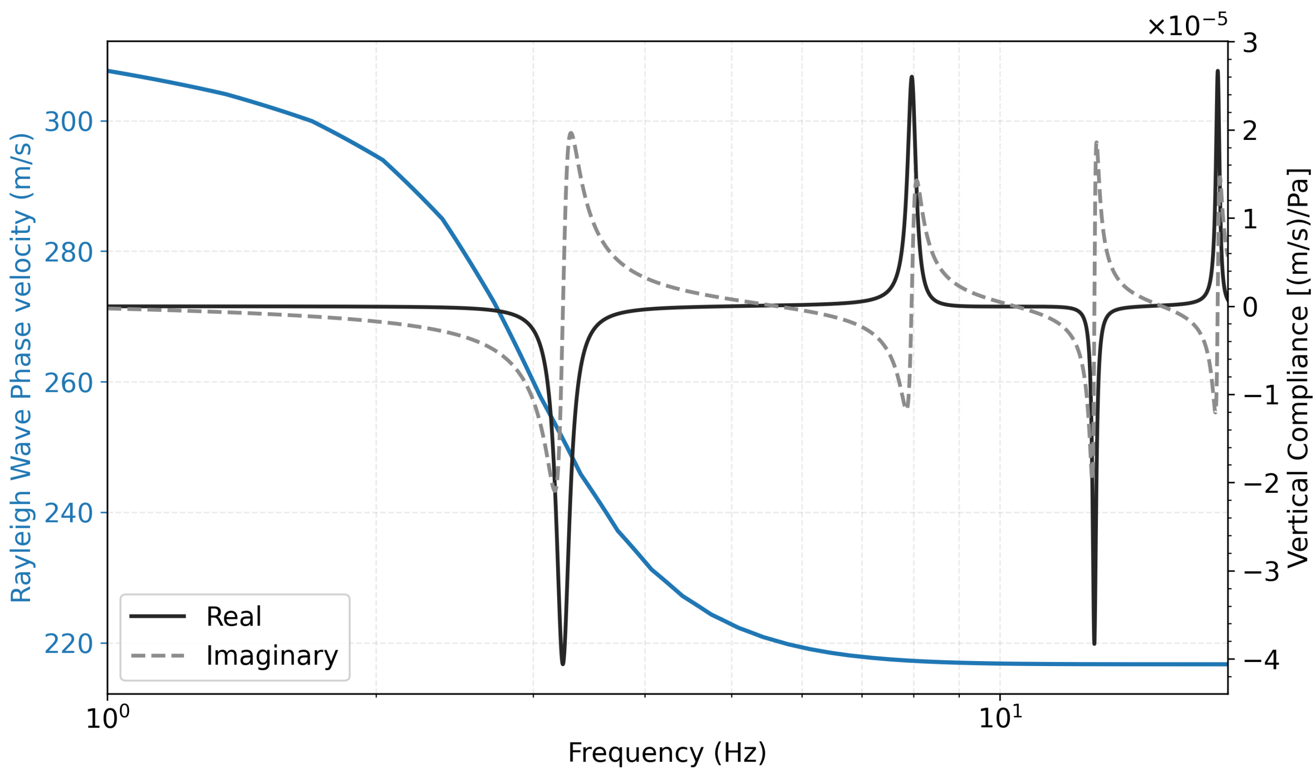

Figure S6 Rayleigh wave phase velocity (blue line) and vertical compliance (black and gray) using median posterior parameters in Supplemental Figure S4 for a layer over halfspace subsurface model. Notice that the Rayleigh wave phase velocity does not match the acoustic apparent velocity (≈345 m/s) when the dominant coupling activation frequency occurs at ≈3.2 Hz. This suggests that air-coupled Rayleigh wave was not activated here, but rather a leaky-mode surface wave is present.

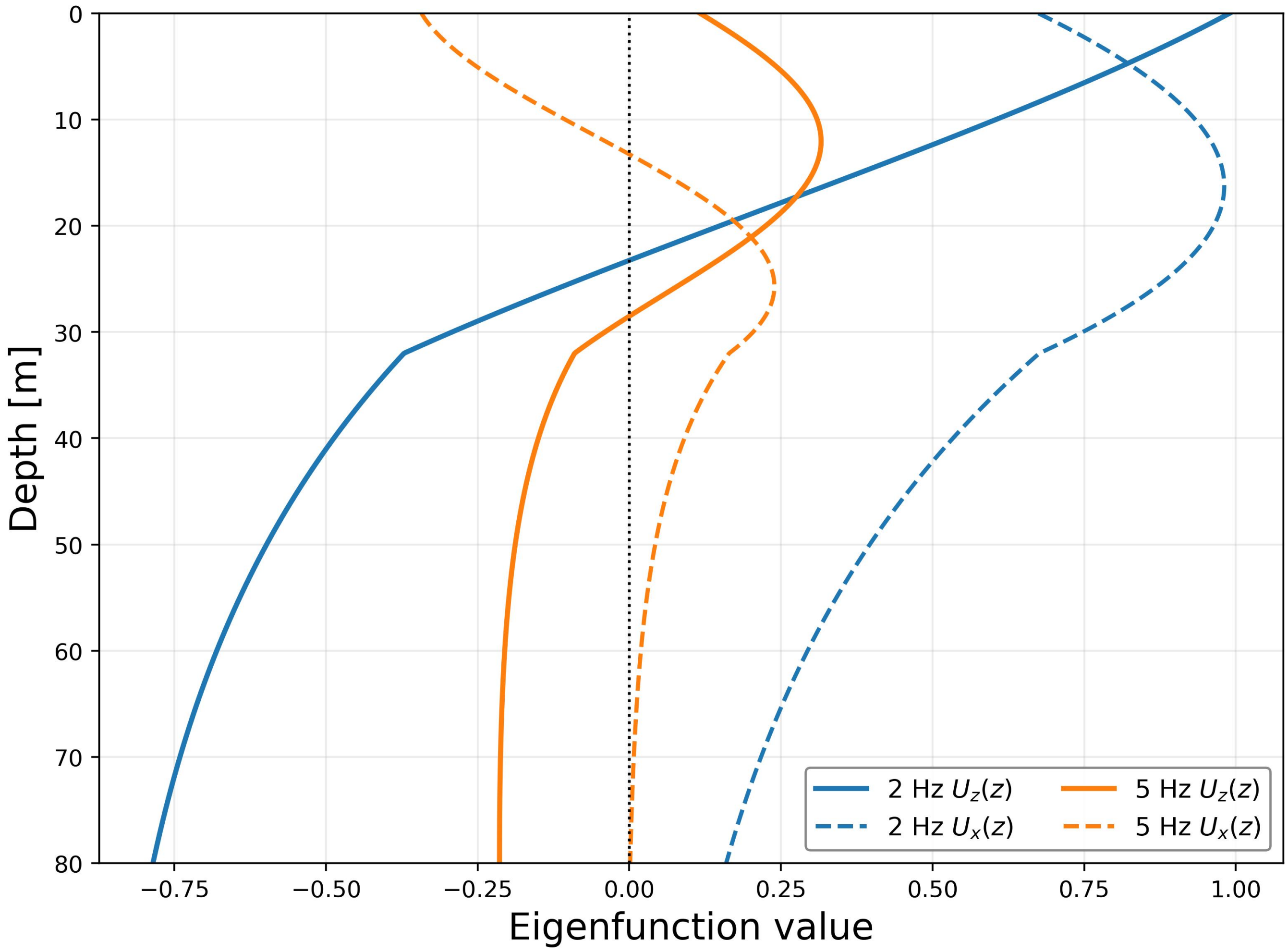

Figure S7 Real part of the eigenfunctions computed for the best-fitting subsurface model from Figure 8 in the main text. Vertical (solid line) and horizontal (dashed line) displacement eigenfunctions at 2 Hz (blue) and 5 Hz from the surface to a depth of 80m. Note the change in sign of the surface horizontal eigenfunction between 2 and 5 Hz.